Protein Science (1996), 5:2333–2342. Cambridge University Press. Printed in the USA.

Evidence for an active T-state pig kidney fructose 1,6-bisphosphatase: Interface residue Lys-42 is important for allosteric inhibition and AMP cooperativity

GUQIANG LU, BOGUSLAW STEC, EUGENE L. GIROUX,[1] AND EVAN R. KANTROWITZ

Department of Chemistry, Merkert Chemistry Center, Boston College, Chestnut Hill, Massachusetts 02167

(RECEIVED July 31, 1996; ACCEPTED August 26, 1996)

Abstract

During the R → T transition in the tetrameric pig kidney fructose-1,6-bisphosphatase (Fru-1,6-P_2ase, EC 3.1.3.11) a major change in the quaternary structure of the enzyme occurs that is induced by the binding of the allosteric inhibitor AMP (Ke HM, Liang JY, Zhang Y, Lipscomb WN, 1991, *Biochemistry 30*:4412–4420). The change in quaternary structure involving the rotation of the upper dimer by 17° relative to the lower dimer is coupled to a series of structural changes on the secondary and tertiary levels. The structural data indicate that Lys-42 is involved in a complex set of intersubunit interactions across the dimer–dimer interface with residues of the 190's loop, a loop located at the pivot of the allosteric rotation. In order to test the function of Lys-42, we have replaced it with alanine using site-specific mutagenesis. The k_{cat} and K_m values for Lys-42 → Ala Fru-1,6-P_2ase were 11 s^{-1} and 3.3 μM, respectively, resulting in a mutant enzyme that was slightly less efficient catalytically than the normal pig kidney enzyme. Although the Lys-42 → Ala Fru-1,6-P_2ase was similar kinetically in terms of K_m and k_{cat}, the response to inhibition by AMP was significantly different than that of the normal pig kidney enzyme. Not only was AMP inhibition no longer cooperative, but also it occurred in two stages, corresponding to high- and low-affinity binding sites. Saturation of the high-affinity sites only reduced the activity by 30%, compared to 100% for the wild-type enzyme. In order to determine in what structural state the enzyme was after saturation of the high-affinity sites, the Lys-42 → Ala enzyme was crystallized in the presence of Mn^{2+}, fructose-6-phosphate (Fru-6-P), and 100 μM AMP and the data collected to 2.3 Å resolution. The X-ray structure showed the T state with AMP binding with full occupancy to the four regulatory sites and the inhibitor Fru-6-P bound at the active sites. The results reported here suggest that, in the normal pig kidney enzyme, the interactions between Lys-42 and residues of the 190's loop, are important for propagation of AMP cooperativity to the adjacent subunit across the dimer–dimer interface as opposed to the monomer–monomer interface, and suggest that AMP cooperativity is necessary for full allosteric inhibition by AMP.

Keywords: allostery; metalloenzymes; protein structure–function; site-specific mutagenesis; X-ray diffraction

Fructose 1,6-bisphosphatase (EC.3.1.3.11) catalyzes the hydrolysis of fructose 1,6-bisphosphate to fructose 6-phosphate and inorganic phosphate, a key control step in the gluconeogenesis pathway. Most Fru-1,6-P_2ases are homotetramers and require divalent metals for activity. The most detailed structural data are currently available for the pig kidney enzyme, which has 337 amino acids per subunit (Marcus et al., 1982; Williams & Kantrowitz, 1992). For the pig kidney enzyme, structures have been determined for the unliganded enzyme (Ke et al., 1989b) and for complexes of this enzyme with the product Fru-6-P (Ke et al., 1991b), with the inhibitor AMP (Ke et al., 1991a), and with the inhibitor Fru-2,6-P_2 (Ke et al., 1989a), among others (for a recent review see Liang et al., 1992). The tertiary structure of each subunit is divided into two folding domains, the AMP and the Fru-1,6-P_2 domains (Fig. 1). The AMP binding site of each subunit is approximately 30 Å distant from the active site (Ke et al., 1991a) and the metal-binding sites are located between the Fru-1,6-P_2 and AMP domains (Ke et al., 1990).

Although Fru-1,6-P_2ase is an allosteric enzyme, kinetic data suggest that it is normally in the active R state. The binding of AMP induces the structural and functional conversion of the en-

Reprint requests to: Evan R. Kantrowitz, Department of Chemistry, Merkert Chemistry Center, Boston College, Chestnut Hill, Massachusetts 02167; e-mail: evan.kantrowitz@.bc.edu.

[1] Present address: Division of Pharmacology and Medicinal Chemistry, University of Cincinnati Medical Center, 3223 Eden Ave, Cincinnati, Ohio 45267-0004.

Abbreviations: Fru-1,6-P_2ase, fructose-1,6-bisphosphatase; Fru-1,6-P_2, fructose 1,6-bisphosphate; Fru-2,6-P_2, fructose 2,6-bisphosphate; Fru-6-P, fructose 6-phosphate; Lys-42 → Ala, the mutant pig kidney fructose-1,6-bisphosphatase with alanine in place of lysine at position 42; RMSD, RMS displacement.

$$R_{\text{merge}} = \frac{\sum_{hkl}\sum_{i}|I_{mean} - I_i|}{\sum_{hkl}\sum_{i} I_i} \qquad R = \frac{\sum|F_{Obs} - F_{Calc}|}{\sum F_{Obs}}$$

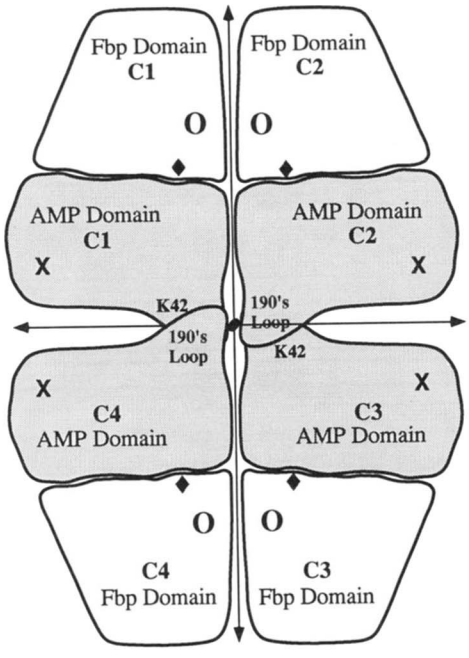

Fig. 1. Schematic representation of the quaternary structure of fructose 1,6-bisphosphatase viewed down a molecular twofold axis. Each of the subunits is composed of two folding domains. The AMP domain has the AMP binding site (X), and the fructose 1,6-P_2 (Fbp) domain contains the active site (O). Divalent metal sites are located between the AMP and Fbp domains (◆). Residues of the 190's loop make critical contacts with Lys-42 (K42).

zyme into the inactive T state. The enzyme requires divalent metal cations such as Mg^{2+}, Mn^{2+}, or Zn^{2+} for catalytic activity, and there are two metal binding sites per subunit. The substrate saturation curve is hyperbolic, although substrate inhibition is observed at sufficiently high substrate concentrations. Furthermore, a plot of reaction velocity versus concentration of magnesium is sigmoidal (Nimmo & Tipton, 1975). One of the metal binding sites is considered a structural site because the metal at this site is thought to be essential for substrate binding, whereas the other metal binding site is considered a catalytic metal site because it is important for catalysis. The enzyme is competitively inhibited by fructose 2,6-bisphosphate, which binds to the substrate binding sites, and allosterically inhibited by AMP, which binds cooperatively to the allosteric sites.

On the basis of the crystal structures of the R (Ke et al., 1991b) and the T (Ke et al., 1991a) allosteric states, Lipscomb and coworkers have proposed structural details concerning the allosteric transition in pig kidney Fru-1,6-P_2ase. The R → T transition of pig kidney Fru-1,6-P_2ase involves a 17° rotation of the C1:C2[2] dimer with respect to the C3:C4 dimer. During the transition, the Fru-1,6-P_2 domain maintains not only its internal structure, but also its interactions with the neighboring subunit. However, dramatic changes occur both within each AMP domain and in the interactions of this domain with its neighboring AMP domains (see Fig. 1). Zhang et al. (1994) have proposed that small initial changes in any one of the AMP domains are propagated quickly and efficiently to other parts of the molecule through the concerted movement of neighboring AMP domains.

Structural data suggest that the interactions involving the 190's loops and Lys-42 residues, near the molecular symmetry axes, are critical for the R → T transition in the pig kidney enzyme because these loops act as a molecular ball and socket for the semi-rigid body rotation around the molecular twofold axis (Zhang et al., 1994). Highly conserved residues of the 190's loop,[3] such as Gly-191 and Glu-192, form stabilizing interactions with Lys-42 of the AMP domain at the dimer–dimer interface. These C1:C4 or C2:C3 interactions are observed in the structures of both the R and T states (Zhang et al., 1994). Lys-42 was replaced by Ala in pig kidney Fru-1,6-P_2ase in order to investigate (1) the relationship between the cooperative binding of AMP and allosteric inhibition at the active site, (2) the relative importance of the C1:C2 versus C1:C4 pathways between subunits for AMP cooperativity, and (3) the relative importance of global versus direct pathways for AMP inhibition. The mutant Fru-1,6-P_2ase (Lys-42 → Ala) was expressed in *Escherichia coli*, and the consequences of this mutation on the structural and functional properties of the enzyme were examined.

Results

Kinetic properties of the Lys-42 → Ala Fru-1,6-P_2ase

Purified enzymes were used to measure all the kinetic parameters. Because both the wild-type and the Lys-42 → Ala enzymes exhibited substrate inhibition at high substrate concentrations, analysis of the kinetic data for both enzymes was performed using a nonlinear least squares method incorporating a term for substrate inhibition. The Lys-42 → Ala enzyme had both a lower V_{max} and a higher K_m compared to the corresponding values for the wild-type enzyme (Fig. 2). The V_{max} of the Lys-42 → Ala Fru-1,6-P_2ase was 17.6 $\mu mol \cdot min^{-1} \cdot mg^{-1}$, which is twofold lower than the corresponding value for wild-type enzyme (34 $\mu mol \cdot min^{-1} \cdot mg^{-1}$) (see Table 1). The decreased catalytic efficiency of the mutant enzyme was also reflected in an approximate twofold increase in the K_m, which was 3.3 μM for the Lys-42 → Ala compared to 1.4 μM for the wild-type enzyme.

Influence of Mg^{2+} on the wild-type and mutant enzymes

Wild-type Fru-1,6-P_2ase requires divalent metal cations, such as Mg^{2+}, to achieve catalytic activity. Magnesium activation for both the wild-type and the Lys-42 → Ala enzymes was cooperative, with a Hill coefficient of approximately 2. However, the concentration of Mg^{2+} required to activate the wild-type enzyme to half of its maximal activity was 0.34 mM, compared to 0.64 mM needed for the Lys-42 → Ala enzyme (Table 1). Therefore, the Lys-42 → Ala Fru-1,6-P_2ase required more Mg^{2+} to be activated to the same extent as the wild-type enzyme.

Influence of Fru-2,6-P_2 on the wild-type and mutant enzymes

Fru-2,6-P_2 is a competitive inhibitor for both the wild-type and the Lys-42 → Ala Fru-1,6-P_2ases. However, the K_i for Fru-2,6-P_2 of the Lys-42 → Ala enzyme was 0.084 μM, slightly higher than the value observed for the wild-type enzyme (0.065 μM).

[2] The four subunits of Fru-1,6-P_2ase are designated C1, C2, C3, and C4, and labeled clockwise (see Fig. 1). The C1 and C2 subunits correspond to the upper dimer and the C3 and C4 subunits correspond to the lower dimer. Therefore, C4 is below C1 and C3 is below C2 (for additional details see Ke et al., 1991a).

[3] The 190's loop corresponds to residues 184–193 in the AMP domain.

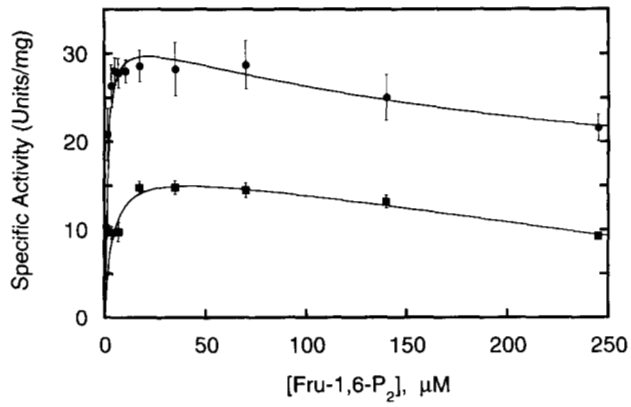

Fig. 2. Dependence of the activity of wild-type (●) and the Lys-42 → Ala (■) Fru-1,6-P_2ases on the concentration of Fru-1,6-P_2 at 2 mM Mg^{2+}. Assays were performed in Tris buffer, pH 7.5, at 30 °C. All data points are the average of at least four determinations. Error bars indicate ±1 SD, and the curves drawn are the best-fit curves calculated by a nonlinear least-squares procedure to the Michaelis–Menten equation incorporating a term for substrate inhibition.

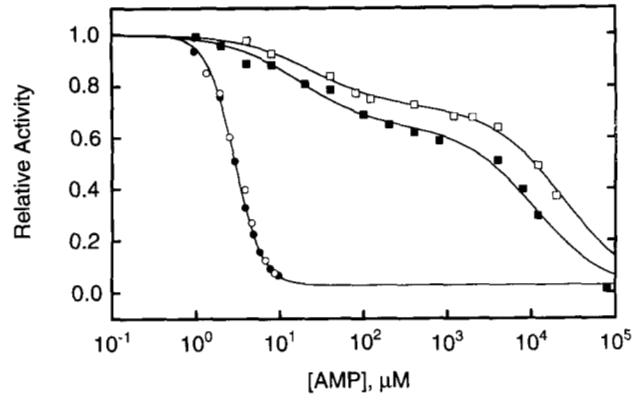

Fig. 3. Inhibition of the wild-type and the Lys-42 → Ala Fru-1,6-P_2ases by AMP at two concentrations of Fru-1,6-P_2 expressed as activity relative to inhibitor-free rates, at 2 mM Mg^{2+}. Data are shown for the wild-type enzyme at 35 μM (●) and 350 μM (○) Fru-1,6-P_2 and the Lys-42 → Ala enzyme at 35 μM (■) and 350 μM (□) Fru-1,6-P_2. Assays were performed under the same conditions described in the legend to Figure 2.

Influence of AMP on the wild-type and mutant enzymes

AMP is an allosteric inhibitor of wild-type Fru-1,6-P_2ase and the inhibition of the enzyme is cooperative, with a Hill coefficient of approximately two. The influence of AMP on the Lys-42 → Ala enzyme is completely different from that observed for the wild-type enzyme. As seen in Figure 3, the inhibition is biphasic, suggesting two classes of binding sites with significantly different affinity for AMP. Furthermore, the binding of AMP to both classes of sites occurs with no cooperativity. During the first phase of AMP inhibition, the Lys-42 → Ala enzyme is inhibited by AMP concentrations less than 100 μM, about 30%. At 1,000-fold higher concentrations of AMP, the mutant enzyme is fully inhibited when both the high- and low-affinity sites are saturated. Based on an analysis of the AMP inhibition curve of the Lys-42 → Ala enzyme determined at 35 μM Fru-1,6-P_2, the dissociation constant for the high-affinity class of AMP sites is 17.8 ± 4.0 μM compared to 2.8 μM for the single class of sites in the wild-type enzyme. Under the same conditions, the dissociation constant for the second class of sites of the Lys-42 → Ala enzyme was 10.9 ± 1.6 mM, corresponding to approximately 600-fold weaker binding compared to the high-affinity sites. The affinity of AMP for the Lys-42 → Ala enzyme was also determined at a 10-fold higher substrate concentration, 350 μM. Under these conditions, the AMP dissociation constants were 22.5 ± 4.0 μM and 23.3 ± 1.7 mM for the high- and low-affinity sites, respectively. Although a 10-fold increase in substrate concentration did not influence the binding affinity of AMP for the wild-type enzyme (see Fig. 3) and for the high-affinity sites in the Lys-42 → Ala enzyme, it did cause a twofold increase in the dissociation constant for the low-affinity sites in the mutant enzyme.

Structure determination of the Lys-42 → Ala Fru-1,6-P_2ase

In order to evaluate the structural alteration induced by AMP when only the high-affinity binding sites have been filled, the Lys-42 → Ala enzyme was crystallized in the presence of 100 μM AMP, 1.0 mM Fru-6-P, and 250 μM Mn^{2+}. As seen in Figure 3, most of the high-affinity AMP sites should be filled at this AMP concentration. The enzyme crystallized in the space group $P2_12_12$ with an unit cell of a = 61.05 Å, b = 166.72 Å, c = 79.98 Å, which is characteristic of the T-state (Ke et al., 1990). The refinement of the structure was initiated with the model of the Arg-243 → Ala mutant of Fru-1,6-P_2ase (PDB file: 1rdz, Bernstein et al., 1977), with ligands and water molecules removed. The structure of the Arg-243 → Ala Fru-1,6-P_2ase used was in the T state refined at 2.05 Å resolution to an R-factor of 19.7% (Stec et al., 1996), with Lys-42 replaced with alanine and the original Arg-243 restored. The model

Table 1. *Kinetic parameters for wild-type and Lys-42 → Ala Fru-1,6-P_2ases*[a]

Enzyme	k_{cat} (s^{-1})	K_m, Fru-1,6-P_2 (μM)	$[Mg^{2+}]_{0.5}$[b] (mM)	K_{app},[c] AMP (μM)	K_i, Fru-2,6-P_2 (μM)
Wild-type	21 ± 1	1.4 ± 0.3	0.34	2.8 μM	0.065 ± 0.005
Lys-42 → Ala	10.8 ± 0.5	3.3 ± 0.7	0.64	18 μM; 11 mM	0.084 ± 0.008

[a]Experiments on wild-type and Lys-42 → Ala enzymes were performed at 17.5 μM Fru-1,6-P_2 and 2 mM magnesium when the components were held constant, except as noted.

[b]Concentration of Mg^{2+} required to activate the enzyme half of the maximal extent.

[c]Apparent dissociation constant for AMP to the single class of sites on the wild-type enzyme or to the high- and low-affinity binding sites of the Lys-42 → Ala enzyme. Data were collected at 35 μM fru-1,6-P_2.

Table 2. *Refinement statistics for the refined model of fru-1,6-P_2ase Lys-42 → Ala mutant enzyme*

Final *R*-factor	d_{min} (Å)	Ligands (occupancy) [temp. factor]	No. of water molecules	RMS deviations: Bond lengths (Å)	RMS deviations: Bond angles (°)	RMS deviations: Improper dihedral angles (°)
0.184	2.3	2 × Fru-6-P (1.0), [34.6] 2 × AMP (1.0), [23.7]	118	0.012	1.87	1.54

of the Lys-42 → Ala Fru-1,6-P_2ase in the T state refined well to a final *R*-factor of 18.4%, with excellent geometry (Table 2). The quality of the structure was monitored using the program PROCHECK (Laskowski et al., 1993). All of the statistics of the final structure were within acceptable limits compared to other structures at similar resolution. The backbone torsional angles were well within allowed regions of the Ramachandran plot (not shown) and side-chain torsional angles were tightly clustered around allowed conformers. The final refinement statistics are presented in Table 2. The Luzzati plot (Luzzati, 1952) for the T state structure indicated a positional error of ±0.25 Å.

The structure of the Lys-42 → Ala enzyme shows relatively little divergence from other T state structures of the wild-type enzyme (Ke et al., 1990, 1991a; Xue et al., 1994). The RMSDs between the final model and the initial Arg-243 → Ala structure (PDB code 1RDZ) were 0.36 Å for the backbone atoms and 0.57 Å for the side-chain atoms, respectively.

Active site

The inhibitor Fru-6-P bound in the active site, with occupancy 1.0 and temperature factors comparable to that of the neighboring residues, was clearly visible in the electron density maps and its positioning is unambiguous. The phosphate group of the inhibitor is held by numerous hydrogen bonds (Fig. 4) to Tyr-215, Asn-212, Tyr-244, Tyr-264, Lys-274, and the O3 oxygen of the furanose ring to the amide nitrogen of Met-248 and carboxyl group of Asp-121 in the very same manner as in the wild-type enzyme (Ke et al., 1990).

At each active site, a distinct peak for one metal ion was detected. Because we used Mn salts in the crystallization, Mn^{2+} ions were used in the refinement. The metal ions show a distinct trigonal bipyramidal coordination, reminiscent but different from that found in the wild-type enzyme (Ke et al., 1990). In the site refined previously as harboring a second metal ion (Zhang et al., 1993), a water molecule was refined instead, as suggested by the temperature factors and the distances to the protein ligands.

Allosteric site and AMP binding

In the T-state structure of the Lys-42 → Ala enzyme, one AMP molecule was found in each of the two chains of the dimer that comprise the asymmetric unit. The structure of the mutant enzyme showed unchanged AMP binding at the regulatory site compared to the wild-type enzyme. The AMP molecule refined with full occupancy and the resulting temperature factors were slightly lower than neighboring residues. The phosphate group had well-defined interactions with backbone nitrogens of residues Thr-27, Gly-28, Glu-29, and Met-30 and side chains of Thr-27, Lys-112 and Tyr-113, which also interacts with O3′ of the ribose ring. Both ribose oxygens are within hydrogen bonding distance of guanidinium nitrogens of Arg-140. Both AMP adenosine rings are in the *anti* conformation, with two distinct hydrogen bonds to the side chain of Thr-31 and the carbonyl oxygen of Val-17 to the N6 nitrogen of the adenine ring (Fig. 5).

Dimer–dimer interface and Lys-42

As expected for the mutant enzyme, there was no detectable difference density corresponding to the presence of the Lys-42 at the dimer–dimer interface in the refined T-state structure. The side-chain conformation of Glu-192 changed from (180, −60) to (−60, +60), resulting in a carboxylate position approximately the same as observed in the wild-type enzyme. The surprising result is that the overall changes at the interface are small and that the Glu-192, which in the wild-type enzyme is involved in a salt bridge with Lys-42, did not change its conformation radically (Fig. 6). A much larger change could be expected upon deletion of the two charged Lys-42 residues positioned in close vicinity to each other in the wild-type enzyme (Fig. 7). A large well-formed water cluster was observed at the dimer interface comprising 13 water molecules in the vicinity of the missing amino groups of the Lys-42 (Fig. 6).

Discussion

In a comparison of the R and T state X-ray crystal structures of Fru-1,6-P_2ase, Zhang et al. (1994) found that, during the R → T transition, the upper dimer (C1:C2) rotates about 17° relative to the lower dimer (C3:C4). Furthermore, during the R → T transition, the Fru-1,6-P_2 domains of each subunit maintain their internal conformation and their mutual interactions within the (C1:C2) dimer, but significant changes occur within the AMP domains of each subunit. The AMP domain of each subunit rotates about 1.0° and translates about 1.6 Å relative to the Fru-1,6-P_2 domain. Because of the relative movements between the Fru-1,6-P_2 and the AMP domains during the R → T transition, the position of the second metal site (M_2) is altered. Villeret et al. (1995) proposed that this displacement of the metal ion at the M_2 site (~1.4 Å) is sufficient to cause inactivation of the enzyme because in the T state position, the M_2 metal cannot function catalytically in the hydrolysis reaction.

In wild-type Fru-1,6-P_2ase, Lys-42 forms intersubunit interactions at the dimer–dimer interface between the C1 and C4 sub-

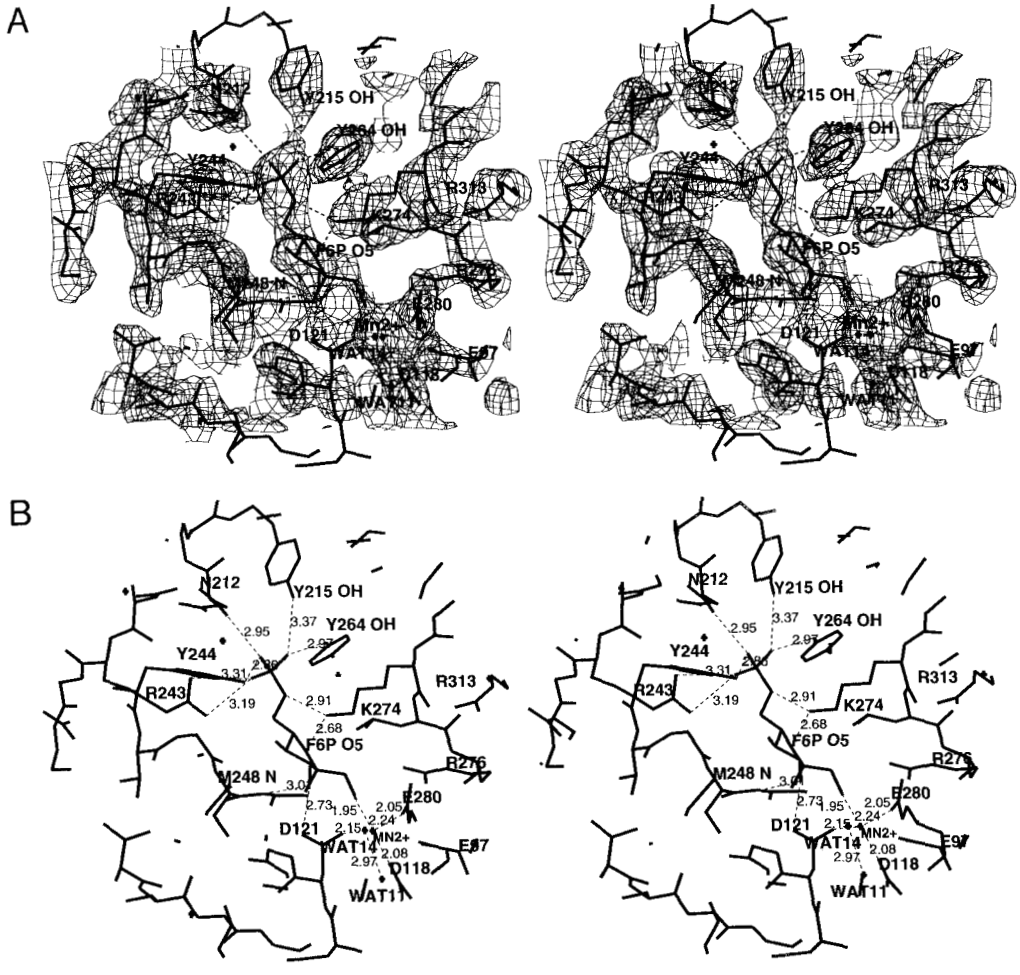

Fig. 4. Stereo view of active site of pig kidney Fru-1,6-P_2ase in the T state with the inhibitor Fru-6-P (B = 38.2 Å^2) and the Mn^{2+} metal ion bound (B = 49.1 Å^2) (**A**) with the $2F_o - F_c$ electron density, which was contoured at the 1.3σ level, superimosed on the atomic coordinates of the refined model; (**B**) the bond-stick model with the network of hydrogen bonds involved in binding the product/inhibitor and the metal ion. Residues involved in Fru-6-P and metal ion binding are labeled.

units, where Lys-42 (C1) interacts with Ile-190 (C4), Gly-191 (C1), and Glu-192 (C4), all located within the 190's loops (see Fig. 7). Here, we have investigated the molecular mechanism of cooperativity in Fru-1,6-P_2ase by using site-specific mutagenesis to probe the functional role of Lys-42 and X-ray crystallography to probe the structural consequences of the mutation.

When Lys-42, which is approximately 30 Å from the active site, was replaced with Ala, the catalytic function of the enzyme was not altered significantly nor was the binding of the competitive inhibitor Fru-2,6-P_2. Magnesium binding was still cooperative; however, the binding affinity of magnesium was approximately twofold lower than that observed for the wild-type enzyme. The X-ray structure supports these kinetic observations, showing the same organization of the active site with the inhibitor Fru-6-P and one metal ion bound.

Lys-42 → Ala enzyme interacts with AMP differently than the wild-type enzyme

The most significant alteration caused by the Lys-42 → Ala substitution involved a change in the affinity and mode by which AMP interacts with Fru-1,6-P_2ase. Not only is the binding affinity of AMP reduced for the Lys-42 → Ala enzyme, but also there is no cooperativity associated with its binding. Furthermore, the binding of AMP to the Lys-42 → Ala enzyme is biphasic with high-affinity and low-affinity components (see Fig. 4). The inhibition of the enzyme is total only when both classes of binding sites are occupied. When the high-affinity sites are saturated, the enzyme still retains approximately 70% activity. The high-affinity sites are characterized by an apparent binding constant that is independent of the substrate concentration, whereas the apparent binding constant for the low-affinity sites increases when the concentration of substrate is increased.

The X-ray structure showed that the mode of binding of AMP to the Lys-42 → Ala enzyme at the regulatory sites was almost identical to that observed for the wild-type enzyme. All crucial interactions of the phosphate, ribose, and adenosine are conserved. The occupancy in conjunction with the temperature factors also suggests that the binding of AMP at the allosteric site is very similar to that in the wild-type enzyme.

The kinetic data combined with the unchanged mode of AMP binding observed in the X-ray structure of the Lys-42 → Ala

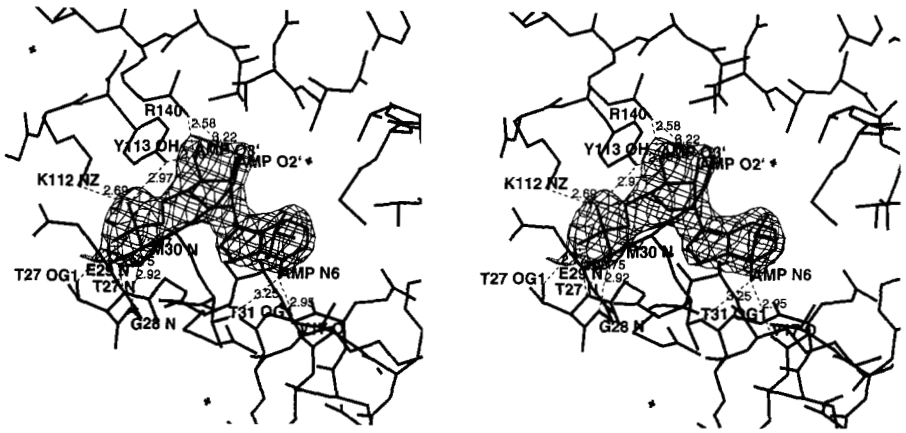

Fig. 5. Stereo view of the effector binding site. Electron density, contoured as in the Figure 4, covers the bound AMP molecule. Residues involved in AMP binding are labeled and hydrogen bonds are also indicated. AMP molecules were refined with full occupancy and temperature factors 26.3 Å^2 in the C1 and 19.1 Å^2 in the C2 subunits, respectively, which is fully comparable to the overall protein temperature factor (B = 24.3 Å^2).

enzyme suggest that the high-affinity AMP sites are the allosteric sites to which AMP normally binds, whereas the low-affinity AMP sites are the active sites. Because of the structural similarities between AMP and the substrate Fru-1,6-P_2, it would be expected that AMP would have some affinity for the active site of Fru-1,6-P_2ase. However, the binding of AMP to the active sites of wild-type Fru-1,6-P_2ase would not be detected by standard activity measurements because the enzyme is completely inactivated by concentrations of AMP that would be insufficient to bind significantly to the active sites. This is not the case for the Lys-42 → Ala enzyme, because the binding of AMP to the regulatory sites does induce the conversion of the enzyme to the T state, but does not fully inactivate the enzyme. Therefore, the influence of high levels of AMP binding competitively at the active site can be discerned, and would explain why increasing the concentration of substrate influences the binding of AMP to the low-affinity but not the high-affinity class of sites.

Evidence for an active T-state of the Lys-42 → Ala Fru-1,6-P_2ase

For wild-type Fru-1,6-P_2ase, saturation of the regulatory sites by AMP functionally causes complete inactivation of the enzyme and structurally causes the conversion of the enzyme into the T-state structure. The Lys-42 → Ala enzyme was crystallized under conditions that would saturate the high-affinity binding sites, but not populate significantly the low-affinity sites. In this fashion, it was possible to determine the quaternary structure of the mutant enzyme and the location of the high-affinity binding sites.

The structure of the Lys-42 → Ala enzyme revealed that the enzyme had the T-state quaternary structure and that the regulatory sites were 100% occupied by AMP. These data indicate that the high-affinity binding sites observed kinetically were indeed the regulatory sites. The kinetic data, indicating that when the high-affinity sites are fully occupied the enzyme still retains approximately 70%

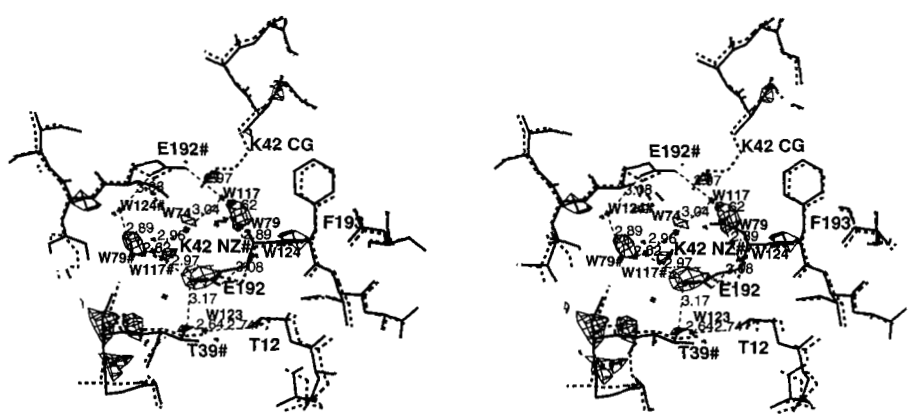

Fig. 6. Stereo view of the C1:C4 interface of pig kidney Fru-1,6-P_2ase in the T state as refined in the mutant Lys-42 → Ala (thick line) superimposed onto the model of the Arg-243 → Ala (thick broken line) from which the refinement was initiated. The difference density is contoured at 2.5σ. Shown are portions of helix H2 and the 190's loop of subunits C1 and C4. The density clearly indicates the absence of Lys-42, the position of which is taken by a cluster of water molecules (labeled crosses). Unlabeled crosses indicate water molecules found in the Arg-243 → Ala mutant. Note the two small conformational changes to residues Glu-192 and Phe-193. The overall positioning of the secondary structure elements seem unchanged as indicated by the model of a mutant structure Arg-243 → Ala (in thick broken lines), which was found to be isostructural with the wild-type enzyme (RMSD 0.37 Å) and showed no loss of cooperativity in AMP binding (Stec et al., 1996).

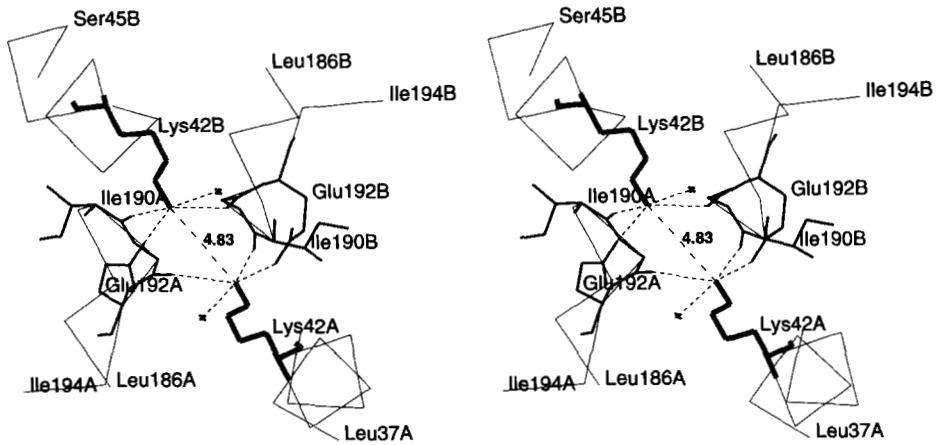

Fig. 7. Stereo view of the C1:C4 interface of pig kidney Fru-1,6-P_2ase in the R state (drawn with Protein Data Bank file 5fbp; Ke et al., 1991a). Shown are portions of helix H2 (residues Leu-37–Thr-46) and the 190's loop (residues Leu-186–Ile-194) of subunits C1 and C4. Residues from the C1 and C4 subunits are labeled with A and B, respectively, appended to their numbers. A series of interactions occurs between Lys-42 and carbonyl oxygens Ile-190 and Gly-191, as well as a salt-link to the carboxylate of Glu-192. These interactions help neutralize the positive charges of the two Lys-42 residues (C1 and C4), allowing them to approach within 4.83 Å of each other.

activity, and the structural data, indicating that the Lys-42 → Ala enzyme is in the T-state, when taken together, provide evidence that the Lys-42 → Ala enzyme can exist in a T-state quaternary structure that still has activity, but does not have cooperative AMP binding.

Villeret et al. (1995) proposed that the mechanism of inhibition by AMP is due to the displacement of metal ion at the M_2 binding site. Both metal ion binding sites (M_1, M_2) in the mutant enzyme were compared to the corresponding sites in the wild-type enzyme (Ke et al., 1990). Little change was observed at the fully occupied M_1 binding site (B = 50 Å^2), and the site was interpreted as being trigonal bipyramidal in symmetry with ligands coming from the protein (Asp-118, Asp-121, Glu-118), O2′ oxygen of the furanose ring, and a water molecule. The relative displacement, however, proved to be small (~0.5 Å), and probably insignificant at the present resolution. The second M_2 binding site was occupied by a water molecule. The position of the M_2 site, however, was not displaced as much as observed by Villeret et al. (1995) for the wild-type enzyme. This more R-like position of the M_2 metal site may be responsible for the residual activity of the Lys-42 → Ala enzyme when the high-affinity AMP site is filled.

The dimer–dimer interface is important for AMP cooperativity

The AMP domains have extensive interactions at both the subunit-subunit interfaces (C1:C2 and C3:C4) and the dimer–dimer interfaces (C1:C4 and C2:C3). Furthermore, most of the conformational changes that happen during the R → T transition occur in the AMP domain. Therefore, it has been proposed that a small initial change at any one of the AMP domains can be propagated quickly and efficiently to other parts of the tetramer to achieve the overall quaternary structural changes (Zhang et al., 1994).

The dimer–dimer interface of Fru-1,6-P_2ase is stabilized by an extensive hydrogen bonding network formed between the AMP domains of the C1 and C4 subunits, as well as the symmetry-related C2 and C3 subunits. During the R → T transition, the rotation of the C1:C2 dimer relative to the C3:C4 dimer results in the breakage of some of the R-state C1:C4 interactions and the formation of new interactions in the T state. One example of this is Arg-22 (C1), which forms interactions with Thr-27 (C4) and Glu-29 (C4) in the T-state and with Glu-108 (C4) and Arg-110 (C4) in the R state (Ke et al., 1991a). When Arg-22 was replaced with alanine, the interaction of the mutant enzyme with AMP was altered. The affinity of the Arg-22 → Ala enzyme for AMP was reduced more than 10-fold; however, AMP binding to the enzyme was still cooperative (Lu et al., 1995).

The interactions involving Lys-42 at the dimer–dimer interface are quite different from those observed for Arg-22 (Ke et al., 1991a). The side chain of Lys-42 (C1) forms intersubunit interactions with backbone carbonyls of Ile-190 (C4), Gly-191 (C1), and the side chain of Glu-192 (C4) (Fig. 7). This complex set of intersubunit interactions involving residues of the 190's loops from both the C1 and C4 subunits is conserved during the R → T transition. The Lys-42 side chains from the C1 and C4 subunits actually point at each other (see Fig. 7) at a very close distance (Ke et al., 1991a). The close approach of these two charge residues is possible by the neutralization afforded Lys-42 by its interactions with nearby groups (Glu-192). This portion of the structure, involving the 190's loops and the Lys-42 residues from the C1 and C4 subunits, has the same conformation in both the R and T states, and may act as a pivot for rotation of the upper dimer relative to the lower dimer (Zhang et al., 1994). The X-ray structure of the mutant showed virtually no change at the C1-C4 interface upon the deletion of Lys-42. Even the conformation of Glu-192 remained similar, suggesting a change in its protonation state; however, one might expect a larger change, as judged by the distribution of charge in this region.

We propose that this portion of the structure also acts as a bridge for the AMP inhibition signal to pass between the two AMP domains across the dimer–dimer interface. Once the interaction between Lys-42 and the 190's loop from the other subunit across the interface is removed, as it is in the Lys-42 → Ala enzyme, the AMP domain of the upper dimer losses its ability to respond to AMP binding to the AMP domain of the lower dimer, and vice versa. This loss of interactions between the two AMP binding domains in the Lys-42 → Ala enzyme may be responsible for the loss of AMP cooperativity in the mutant enzyme.

The importance of the dimer–dimer interface and the tetrameric structure of Fru-1,6-P_2ase

It has long been recognized that there is a synergistic effect between the binding of AMP and the metal cations. Lipscomb and coworkers have proposed that the binding of AMP shifts the position of the second metal binding site (Villeret et al., 1995). This movement of the M_2 site abolishes catalytic activity because the M_2 metal is crucial for activation of the nucleophilic water molecule required for the hydrolysis of Fru-1,6-P_2. Besides the loss of cooperativity for AMP, another significant alteration that results from the Lys-42 → Ala substitution is that the binding of AMP to the allosteric site only inhibits the enzyme by approximately 30%, in contrast to the complete inhibition observed for the wild-type enzyme. Results from the Lys-42 → Ala enzyme, which has lost an interaction at the C1:C4 dimer–dimer interface, suggest that Lys-42 in the tetrameric structure is important in conveying the allosteric signal from the AMP domain to the metal binding site.

Previously, Grazi et al. (1973) studied matrix-bound rabbit liver Fru-1,6-P_2ase as a means to probe the dimer–dimer interface. They found that matrix-bound Fru-1,6-P_2ase became half desensitized to AMP and that the binding of AMP was biphasic. When the high-affinity binding sites were filled with AMP, the matrix-bound enzyme was inhibited by only 40%. Furthermore, the dimer bound to the matrix was almost completely desensitized to AMP, because it could be inhibited by only 13% when the high-affinity sites were filled. These data are consistent with our results, which suggest that the loss of interactions involving Lys-42 decouples those allosteric interactions involving AMP across the dimer–dimer interface. However, the fact that AMP can inhibit the Lys-42 → Ala enzyme by about 30% suggests that the binding of AMP is communicated directly to the M_2 site in the same subunit, but the limitation and the contacts imposed by the entire tetrameric structure are essential for the total inactivation of the enzyme observed upon AMP binding.

Summary

In this paper, we report kinetic as well as crystallographic data for the Lys-42 → Ala Fru-1,6-P_2ase. This mutation shows that it is possible to uncouple the cooperativity of AMP binding and allosteric inhibition. Furthermore, the mutant enzyme can be converted to a T-state quaternary structure that still retains catalytic activity, indicating that the dimer–dimer interface (C1-C4) is responsible for the propagation of the AMP binding and cooperativity. These data also indicate that total inhibition of the enzyme can only be achieved by an integration of inhibition signals over different pathways. These pathways are not local to a single subunit, leading to the conclusion that the entire tetrameric structure is necessary for inhibition. The crystal structure showed that the reason for the altered mode of AMP binding is not a local alteration of the structure around the AMP binding site, but rather the introduction of a defect in one of the important signal transduction pathways between subunits of this multimeric enzyme.

Materials and methods

Materials

Agar, agarose, ampicillin, chloramphenicol, sodium dihydrogen phosphate, and magnesium chloride were purchased from Sigma Chemical Co. Tris and enzyme-grade ammonium sulfate were supplied by ICN Biomedicals. Tryptone and yeast extract were from Difco Laboratories. All the reagents for DNA sequencing were obtained from US Biochemical. Restriction endonucleases, T4 DNA ligase, T4 DNA polymerase, and T4 polynucleotide kinase were from US Biochemical or New England Biolabs, and used according to the supplier's recommendations. DNA fragments were isolated from agarose gels with the Geneclean II kit from Bio 101 Inc.

Strains

The *E. coli* K12 strain MV1190 [Δ(*lac-proAB*), *supE*, *thi*, Δ(*sri-recA*) 306::Tn10(tet^r)/F′ *traD36*, *proAB*, *lacI*^{q}, *lacZ*ΔM15] and the M13 phage M13K07 were obtained from J. Messing. The strain CJ236 [*dut-1*, *ung-1*, *thi-1*, *relA1*/pCJ105(Cm^r)] was a gift of T. Kunkel, and EK1601 [*tonA22*, *ompF627*(T_2^R), *relA1*, *pit-10*, *spoT1*, Δ(*fbp*)287, λDE3], a derivative of DF657 (Sedivy et al., 1984), was constructed in this laboratory (Giroux et al., 1994). *E. coli* strain XL1-Blue MRF$^-$ [Δ(*mcrA*)183, Δ(*mcrCB-hsdSMR-mrr*)172, *endA1*, *supE44*, *thi-1*, *recA*, *gyrA96*, *relA1*, *lac*, λ$^-$/F′ *proAB*, *lacI*^{q}, *lacZ*ΔM15, Tn10(tet^r)] was from Stragene (La Jolla, California).

Oligonucleotide synthesis

Oligonucleotides required for the site-specific mutagenesis and the sequencing primers were synthesized on an Applied Biosystems 381A DNA synthesizer and purified by HPLC employing a DuPont Zorbay Oligo ion-exchange column.

Construction of the expression phagemid pEK284

In order to simplify the construction, and subsequent verification of mutations and expression of mutant Fru-1,6-P_2ases, we modified the plasmid pEK188 (Giroux et al., 1994), which contains the cDNA for pig kidney Fru-1,6-P_2ase. The plasmid pEK188 and the phagemid pET23a (Novagen, Inc.) were cut with *Xba* I and *Xho* I. The fragment containing the cDNA for Fru-1,6-P_2ase was isolated from pEK188 and the larger fragment containing most of the phagemid was isolated from pET23a. These fragments were mixed and treated with T4 DNA ligase. The construction of the resulting phagemid, pEK281, was verified by restriction analysis. Finally, a new *Bam*H I site was introduced into the C-terminal region of the Fru-1,6-P_2ase cDNA by site-specific mutagenesis without altering the amino acid sequence of the protein, creating pEK284. The entire Fru-1,6-P_2ase cDNA coding region in this phagemid was sequenced to verify that no amino acid changes had been introduced.

Construction of the Lys 42 → Ala mutation

Site-specific mutagenesis was performed on the cDNA of Fru-1,6-P_2ase harbored on plasmid pEK284, employing the method of Kunkel et al. (1987). Uracil-containing single-stranded DNA was obtained by infection of *E. coli* strain CJ236 containing pEK284 with helper phage M13KO7 (Vieira & Messing, 1987). Potential mutant candidates were identified initially by DNA sequence analysis (Sanger et al., 1977). The entire cDNA of Fru-1,6-P_2ase of one of these candidates was sequenced to ensure that site-specific mutagenesis had not introduced any additional mutations other than the desired change at amino acid position 42. The resultant plasmid, pEK292, contained only the mutation at the codon corresponding to the Lys-42 → Ala mutation.

Expression of pig kidney Fru-1,6-P_2ase in E. coli

In order to express the wild-type and Lys-42 → Ala pig kidney Fru-1,6-P_2ases, phagemids pEK284 and pEK292, respectively, were transformed into *E. coli* strain EK1601. *E. coli* strain EK1601 has a deletion in the chromosomal *fbp* gene and can be induced to produce T7 RNA polymerase (Giroux et al., 1994). Therefore, the pig kidney Fru-1,6-P_2ase expressed from the plasmid could not be contaminated with the *E. coli* Fru-1,6-P_2ase expressed from the chromosome.

Enzyme purification

Bacteria were cultured with vigorous agitation at 37 °C in M9 medium supplemented with 0.5% casamino acids and ampicillin at 100 μg/mL. Induction of T7 RNA polymerase was initiated by addition of 0.4 mM isopropyl-β-D-thiogalactopyranoside (US Biochemical). After further cultivation for 16–22 h, cells were harvested by centrifugation, then broken open by a freeze–thaw procedure (El-Maghrabi & Pilkis, 1991). The purification of the Lys-42 → Ala enzyme was accomplished by the method described previously (Giroux et al., 1994).

Determination of Fru-1,6-P_2ase activity and data analysis

A spectrophotometric coupled enzyme assay was employed to measure Fru-1,6-P_2ase activity (Riou et al., 1977). Standard conditions (2 mM magnesium chloride, 17.5 μM Fru-1,6-P_2) were used to determine specific activity. Digital absorbance values were collected over a 6-min assay interval and fit to a straight line by computer, using data beyond the coupling lag period. In all assays, the substrate Fru-1,6-P_2 and the enzyme were added last, after incubation and thermal equilibration of the coupling enzymes, magnesium (and inhibitor) components. One unit (U) of enzyme activity causes the reduction of 1 μmol of NADP per minute at 30 °C.

Methods used to determine the kinetic model parameters were described previously (Lu et al., 1995). The AMP inhibition curve of the Lys-42 → Ala Fru-1,6-P_2ase was biphasic and therefore had to be analyzed differently than the data for the wild-type enzyme. The data for both stages exhibited no cooperativity and were therefore fit to the sum of two hyperbolic functions. Multiple determinations of initial rates at a specific set of component concentrations provided measures of assay precision and weighted mean data were used.

Determination of protein concentration

The concentrations of the wild-type and the Lys-42 → Ala enzymes were determined using the Lowry method (Lowry et al., 1951) with bovine serum albumin as the standard.

Other methods

SDS-PAGE was used to judge enzyme homogeneity (Laemmli, 1970). Concentrations of Fru-1,6-P_2 and NADP were checked by performance in the coupled assay of AMP using 15.4 as the millimolar extinction coefficient at pH 7.0 at 259 nm, and of Fru-2,6-P_2 by partial acid hydrolysis and analysis of Fru-6-P (Pilkis et al., 1981).

Crystallization

Concentrated protein was crystallized by the hanging drop vapor diffusion method using conditions established in our laboratory. The crystals grew from a 5-μL solution of 15 mg/mL protein in 50 mM Tris buffer, pH 7.5, mixed with 5 μL of 50 mM Tris buffer, pH 7.5, containing 15% PEG 3500, 180 μM $MnCl_2$, and 0.5 mM EDTA, and suspended over 0.7 mL of the same buffer with 15% PEG 3500. Different additives, such as 1 mM Fru-6-P and/or 100 μM AMP, were also used. The crystals, which grow within 1–2 weeks to typical dimensions of 0.5 × 0.5 × 0.4, were harvested and used directly for data collection.

Data collection and processing

The diffraction data were collected with the Area Detector Systems (San Diego, California) Multiwire Area Detector MARK II system at the Crystallographic Facility in the Chemistry Department of Boston College. The two-area detector system is controlled by a DEC ALPHA 3300 computer. The system is mounted on a Rigaku RU-200 rotating-anode X-ray generator operated at 50 kV and 150 mA. The detectors were positioned at 11° and 30° with crystal to detector distances of 770 mm and 700 mm, respectively. This experimental setup allows the collection of data to 2.2 Å resolution without repositioning the detectors. The data set was collected on a single crystal with overall decay of 16% with 65% completeness to 2.3 Å resolution.

The diffraction data were merged using the software provided by Area Detector Systems (Hamlin et al., 1981). A scale factor was calculated for multiple measurements and symmetry-related reflections. Those measurements deviating substantially from the average for a particular reflection were deleted. This merging and editing procedure was repeated until the R_{merge} converged. Crystal and data collection statistics are presented in Table 3.

Structure refinement

The initial model used to begin the structural refinement was the coordinates of the Arg-243 → Ala mutant of Fru-1,6-P_2ase in the T form (PDB file: 1RDZ), with ligands and water molecules removed. The crystal structure was refined using X-PLOR (Brünger,

Table 3. *Summary of the data collection for the T-state crystal of fru-1,6-P_2ase Lys-42 → Ala mutant enzyme*

Space group	d_{max} (Å)	Reflections total unique	Completeness	Redundancy	Unit cell (Å)	Final R_{merge} (%)
$P2_12_12$	2.3	66,515 27,660	65%	2.5	a = 61.05 b = 166.72 c = 79.98	9.0

1992, Biosym/MSI) running on Silicon Graphics Indigo II workstations at Boston College. The initial *R*-factor was 0.32 for the data better than $2\sigma(F)$ at 2.3 Å. Subsequent positional refinement and temperature-factor refinement improved the *R*-factor and stereochemistry. At this stage, the Fru-6-P and AMP were built according to the calculated electron density $(2F_o - F_c)$ and $(F_o - F_c)$ maps using CHAIN (Sack, 1988). The structures were then further refined by cycles of positional refinement, temperature factor refinement, and simulated annealing using initial temperatures up to 1,000 K.

The solvent water molecules were then added automatically by IMPLOR (T. Tibbitts, unpubl.). During subsequent refinement, the temperature factors of the waters were carefully monitored, and water molecules that had temperature factors above 90 $Å^2$ were deleted. Additional solvent water molecules were added based upon difference Fourier maps $(F_o - F_c)$ at several stages, and 118 waters are present in the final refined structure (Table 2).

The quality of the models were monitored by the program PROCHECK (Laskowski et al., 1993). The molecular fragments 1–8 and 62–70, which usually have very weak electron density and were not previously refined (Ke et al., 1991b), were modeled in and refined in our T-state structure as determined previously in the Arg-243 → Ala mutant (Stec et al., 1996). The electron density for these fragments was weak, but slightly stronger than in the structure of Arg-243 → Ala enzyme. Coordinates for the T state structure of the Lys-42 → Ala Fru-1,6-P_2ase have been deposited with the Brookhaven Protein Data Bank as file 1FSA.

Acknowledgment

This work was supported by grant MCB-9631143 from the National Science Foundation.

References

Bernstein FC, Koetzle TF, Williams GJB, Meyer EF Jr, Brice MD, Rodgers JR, Kennard O, Shimanouchi T, Tasumi M. 1977. The Protein Data Bank: A computer-based archival file for macromolecular structures. *J Mol Biol 112*:535–542.

Brünger AT. 1992. *X-PLOR, version 3.1. A system for crystallography and NMR*. New Haven, Connecticut: Yale University Press.

El-Maghrabi MR, Pilkis SJ. 1991. Expression of rat liver fructose 1,6-bisphosphatase in *Escherichia coli*. *Biochem Biophys Res Commun 176*:137–144.

Giroux E, Williams MK, Kantrowitz ER. 1994. Shared active sites of fructose-1,6-bisphosphatase: Arginine-243 mediates substrate binding and fructose 2,6-bisphosphate inhibition. *J Biol Chem 269*:31404–31409.

Grazi E, Magri E, Traniello S. 1973. Active subunits of rabbit liver fructose diphosphatase. *Biochem Biophys Res Commun 54*:1321–1325.

Hamlin R, Cork C, Howard A, Nielson C, Vernon W, Mathews D, Xuong Nh. 1981. Characteristics of a flat multiwire area detector for protein crystallography. *J Appl Crystallogr 14*:85–93.

Ke HM, Liang JY, Zhang Y, Lipscomb WN. 1991a. Conformational transition of fructose-1,6-bisphosphatase: Structure comparison between the AMP complex (T form) and the fructose 6-phosphate (R form). *Biochemistry 30*:4412–4420.

Ke HM, Thorpe CM, Seaton BA, Lipscomb WN, Marcus F. 1989a. Structure refinement of fructose-1,6-bisphosphatase and its fructose 2,6-bisphosphatase complex at 2.8 Å resolution. *J Mol Biol 212*:513–539 [erratum (1990) *J Mol Biol 214*:950].

Ke HM, Thorpe CM, Seaton BA, Marcus F, Lipscomb WN. 1989b. Molecular structure of fructose-1,6-bisphosphatase at 2.8 Å resolution. *Proc Natl Acad Sci USA 86*:1475–1479.

Ke HM, Zhang Y, Liang JY, Lipscomb WN. 1991b. Crystal structure of the neutral form of fructose-1,6-bisphosphatase complexed with the product fructose 6-phosphate at 2.1 Å resolution. *Proc Natl Acad Sci USA 88*:2989–2993.

Ke HM, Zhang Y, Lipscomb WN. 1990. Crystal structure of fructose 1,6-bisphosphatase complexed with fructose 6-phosphate, AMP and magnesium. *Proc Natl Acad Sci USA 87*:5243–5247.

Kunkel TA, Roberts JD, Zakour RA. 1987. Rapid and efficient site-specific mutagenesis without phenotype selection. *Methods Enzymol 154*:367–382.

Laemmli UK. 1970. Cleavage of structural proteins during the assembly of the head of bacteriophage T4. *Nature (Lond) 227*:680–685.

Laskowski RA, MacArthur MW, Moss DS, Thornton JM. 1993. PROCHECK: A program to check the stereochemical quality of protein structures. *J Appl Crystallogr 26*:283–291.

Liang JY, Zhang Y, Huang S, Ke H, Lipscomb WN. 1992. Activity and allosteric regulation in fructose-1,6-bisphosphatase. *Proc. Robert A. Welch Found. Conf. Chem. Res., 36th (Regulation of Proteins by Ligands)*. Houston: The Robert A. Welch Foundation. pp 57–99.

Lowry OH, Rosebrough NJ, Farr AL, Randell RH. 1951. Protein measurement with folin phenol reagent. *J Biol Chem 193*:265–275.

Lu G, Williams MK, Giroux EL, Kantrowitz ER. 1995. Fructose-1,6-bisphosphatase: Arginine-22 is involved in stabilization of the T allosteric state. *Biochemistry 34*:13272–13277.

Luzzati PV. 1952. Traitement statistique des erreurs dans la determination des structures cristallines. *Acta Crystallogr 5*:802–810.

Marcus F, Edelstein I, Reardon I, Heinrikson RL. 1982. Complete amino acid sequence of pig kidney fructose-1,6-bisphosphatase. *Proc Natl Acad Sci USA 79*:7161–7165.

Nimmo HG, Tipton KF. 1975. The effect of pH on the kinetics of beef-liver fructose bisphosphatase. *Eur J Biochem 58*:567–574.

Pilkis SJ, El-Maghrabi MR, Pilkis J, Claus T. 1981. Inhibition of fructose 1,6-bisphosphatase by fructose 2,6 bisphosphate. *J Biol Chem 256*:3619–3622.

Riou JP, Claus TH, Flockhart DA, Corbin JD, Pilkis SJ. 1977. In vivo and in vitro phosphorylation of rat liver fructose 1,6-bisphosphatase. *Proc Natl Acad Sci USA 74*:4615–4619.

Sack JS. 1988. Chain—A crystallographic modeling program. *J Mol Graph 6*:244–245.

Sanger F, Nicklen S, Coulson AR. 1977. DNA sequencing with chain-terminating inhibitors. *Proc Natl Acad Sci USA 74*:5463–5467.

Sedivy JM, Daldal F, Fraenkel DG. 1984. Fructose bisphosphatase of *Escherichia coli*: Cloning of the structural gene (*fbp*) and preparation of a chromosomal deletion. *J Bacteriol 158*:1048–1053.

Stec B, Abraham R, Giroux EL, Kantrowitz ER. 1996. Crystal Structure of the active site mutant Arg-243 → Ala of pig kidney fructose-1,6-bisphosphatase expressed in *E. coli*. *Protein Sci 5*:1541–1553.

Vieira J, Messing J. 1987. Production of single-stranded plasmid DNA. *Methods Enzymol 153*:3–11.

Villeret V, Huang S, Zhang Y, Lipscomb WN. 1995. Structural aspects of the allosteric inhibition of fructose-1,6-bisphosphatase by AMP: The binding of both the substrate analogue 2,5-anhydro-D-glucitol 1,6-bisphosphate and catalytic metal ions monitored by X-ray crystallography. *Biochemistry 34*:4307–4315.

Williams MK, Kantrowitz ER. 1992. Isolation and sequence analysis of the cDNA for pig kidney fructose 1,6-bisphosphatase. *Proc Natl Acad Sci USA 89*:3080–3082.

Xue Y, Huang S, Liang JY, Zhang Y, Lipscomb WN. 1994. Crystal structure of fructose-1,6-bisphosphatase complexed with fructose 2,6-bisphosphate, AMP, Zn^{2+} at 2.0 Å resolution: Aspects of synergism between inhibitors. *Proc Natl Acad Sci USA 91*:12482–12486.

Zhang Y, Liang JY, Huang S, Ke H, Lipscomb WN. 1993. Crystallographic studies of the catalytic mechanism of the neutral form of fructose-1,6-bisphosphatase. *Biochemistry 32*:1844–1857.

Zhang Y, Liang JY, Huang S, Lipscomb WN. 1994. Toward a mechanism for the allosteric transition of pig kidney fructose-1,6-bisphosphatase. *J Mol Biol 244*:609–624.